Conductivity of SDC and (Li/Na)$_2$CO$_3$ composite electrolytes in reducing and oxidising atmospheres

Andreas Bodén [a,*], Jing Di [b], Carina Lagergren [a],
Göran Lindbergh [a], Cheng Yang Wang [b]

[a] *KTH Chemical Science and Engineering, Applied Electrochemistry, SE-100 44 Stockholm, Sweden*
[b] *School of Chemical Engineering and Technology, Tianjin University, Tianjin 300072, China*

Abstract

Composite electrolytes made of samarium-doped cerium oxide and a mixture of lithium carbonate and sodium carbonate salts are investigated with respect to their structure, morphology and ionic conductivity. The composite electrolytes are considered promising for use in so called intermediate temperature solid oxide fuel cells (IT-SOFC), operating at 400–600 °C. The electrolytes are tested in both gaseous anode (reducing) and cathode (oxidising) environments and at different humidities and carbon dioxide partial pressures. For the structure and morphology measurements, it was concluded that no changes occur to the materials after usage. From measurements of melting energies, it was concluded that the melting point of the carbonate salt phase decreases with decreasing fraction of carbonate salt and that a partial melting occurs before the bulk melting point of the salt is reached. For all the composites, two regions may be observed for the conductivity, one below the carbonate salt melting point and one above the melting point. The conductivity is higher when electrolytes are tested in anode gas than when tested in cathode gas, at least for electrolytes with less than half the volume fraction consisting of carbonate salt. The higher the content of carbonate salt phase, the higher the conductivity of the composite for the temperature region above the carbonate melting point. Below the melting point, though, the conductivity does not follow this trend. Calculations on activation energies for the conductivity show no trend or value that indicates a certain transport mechanism for ion transport, either when changing between the different composites or between different gas environments.
© 2007 Elsevier B.V. All rights reserved.

Keywords: Composite; Electrolyte; Conductivity; SDC; ITSOFC; Fuel cell

1. Introduction

Environmental and economical concerns, such as emissions of greenhouse gases and insufficient oil resources, have during the last decades focussed much attention on fuel cells. In the fuel cell, the chemical energy of a usually gaseous fuel and a gaseous oxidant are directly and continuously converted into electrical energy. Depending on the nature of the fuel cell this conversion takes place at different temperatures using different types of electrolyte. The traditional solid oxide fuel cell (SOFC) operates at temperatures of 800–1000 °C making noble metal catalysts unnecessary. The high operating temperature also enables other fuels than hydrogen to be used in the fuel

cell, e.g. natural gas may be used as a fuel without pre-reforming. Conventional SOFCs use a ceramic oxide electrolyte, typically yttrium-stabilised zirconium (YSZ), which requires the high temperature of 800–1000 °C to obtain a sufficient conductivity of oxygen ions. The high temperature will, however, put restrictions on the materials used in the SOFC, for example, as regards thermo-mechanical properties, life-time and cost. In recent years, a great deal of efforts have been made to reduce the operating temperature of the SOFC below 800 °C, so called intermediate temperature SOFC (ITSOFC). Since the ohmic losses in the SOFC constitute the largest part of the voltage losses, increased conductivities of the cell components and reduced contact resistance between electrodes and electrolyte are the main issues when reducing temperature. Two ways are adopted for this. One is to still use the conventional electrolytes, such as YSZ but making them considerably thinner (see, e.g. Tsai et al. [1]). However, even if making the YSZ electrolyte

* Corresponding author.
  E-mail address: andreas.boden@ket.kth.se (A. Bodén).

very thin it will have large difficulties to meet the demands at intermediate temperatures. A probably more efficient way is to find alternative electrolyte materials that have much higher ionic conductivity than YSZ in the actual temperature range.

Doped cerium oxides (DCO) have been widely investigated and found to be good oxygen ion conductors in the intermediate temperature range [2–4]. A problem with DCOs is their instability in reducing atmosphere, i.e. anode conditions in the fuel cell, in which the Ce^{4+} is reduced to Ce^{3+} [4,5]. This reduction process makes the DCO somewhat electronically conducting, causing a loss in power output of the cell, but it may also lower the mechanical stability of the material. In recent years, composite materials consisting of a salt (most often chloride or carbonate) and DCO have been investigated as electrolytes for ITSOFCs by several researchers [2,6–14]. The DCO salt composites are found to have a suppressed electronic conduction in reducing atmosphere and also to have an enhanced ionic conductivity compared to pure DCO.

In literature most studies of composite materials as electrolyte in ITSOFCs are made in fuel cells and during operation, i.e. together with electrodes and with a fuel-containing gas on the anode and an oxygen-containing gas on the cathode. In this paper, composite electrolytes made of samarium-doped cerium oxide and a mixture of lithium carbonate and sodium carbonate salts are investigated in a symmetrical cell. The symmetrical cell is used to avoid the effects of electrodes and any composition gradients in the electrolyte. The purpose of this study is to elucidate the conducting phase at different temperatures, for different composite compositions and in different gas environments.

2. Experimental

2.1. Preparation of composite electrolyte

A samarium-doped cerium oxide (SDC, $Ce_{0.8}Sm_{0.2}O_{1.9}$) powder was prepared by the sol–gel technique [15]. Stoichiometric amounts of cerium nitride hexahydrate, $Ce(NO_3)_3 \cdot 6H_2O$ (99.9 wt.%, Inner Mongolia Baotou Steel Rare-earth Hitech Co., Ltd., China) and samarium nitride hexahydrate, $Sm(NO_3)_3 \cdot 6H_2O$ (99.9 wt.%, Inner Mongolia Baotou Steel Rare-earth Hi-tech Co., Ltd.) were mixed and dissolved in deionised water. Solid citric acid powder (99.9 wt.%, Merck, Germany) was added to the solution, at a molar ratio of metal ions to citric acid of 1:1.2. The solution was heated and stirred on a hot plate at 70 °C to form a gel. The gel was dried in an oven at 120 °C overnight to remove the water. The dried gel was ground and sintered in air at 850 °C for 5 h to obtain a pure SDC powder.

A mixture of lithium carbonate and sodium carbonate salts $(Li/Na)_2CO_3$ was prepared by mixing Li_2CO_3 (99.9 wt.%, Merck) and Na_2CO_3 (99.9 wt.%, Merck) at a molar ratio of 52/48.

SDC powder and $(Li/Na)_2CO_3$ were mixed and ground thoroughly. The mixture was then heated in air at 600 °C for 0.5 h. The mixture was ground again to obtain a powder. The weight ratios of the composites $(SDC:(Li/Na)_2CO_3)$ were chosen to be 90:10, 80:20 and 50:50, respectively. The name and weight ratio

Table 1
The different composite electrolytes investigated

Composite name	Weight ratio $SDC:(Li/Na)_2CO_3$	Volume ratio $SDC:(Li/Na)_2CO_3$
SDC5050	50:50	25:75
SDC8020	80:20	57:43
SDC9010	90:10	75:25

of each electrolyte is given in Table 1. The volume ratio of each component is calculated from the density of the pure components at room temperature. The calculated density of SDC is $7.12 \, g \, cm^{-3}$ from XRD [16] and the density of the $(Li/Na)_2CO_3$ mixture is $2.35 \, g \, cm^{-3}$ calculated from pure compounds [17]. The electrolyte pellets were prepared by pressing about 1 g powder at a pressure of $1.1 \times 10^7 \, Pa$. The pellets were thereafter sintered at 600 °C for 0.5 h in air.

2.2. Conductivity measurements and experimental setup

The conductivity was measured by using electrochemical impedance spectroscopy (EIS) in a four-probe configuration. The electrolyte was placed between two current collectors covered with gold paste (G3535, Agar Scientific Ltd., England). The current collectors were made of stainless steel, SS316, in the experiments where oxygen containing-gas (cathode gas) was used, while in the case of hydrogen-containing gas (anode gas) current collectors made of nickel were used. The electrolyte package was placed inside a ceramic tube. The setup is schematically shown in Fig. 1. The ceramic tube was placed in an oven. To reduce the contact resistances a mechanical pressure of $6.7 \times 10^4 \, Pa$ was applied.

The setup was heated up to 400 °C over a period of 11 h. During the start-up an N_2/CO_2 (80/20) atmosphere was continuously supplied, to suppress loss of carbonate salt by decomposition of the $(Li/Na)_2CO_3$ [18]. After the heating procedure, the temperature of the oven was manually controlled and the temperature
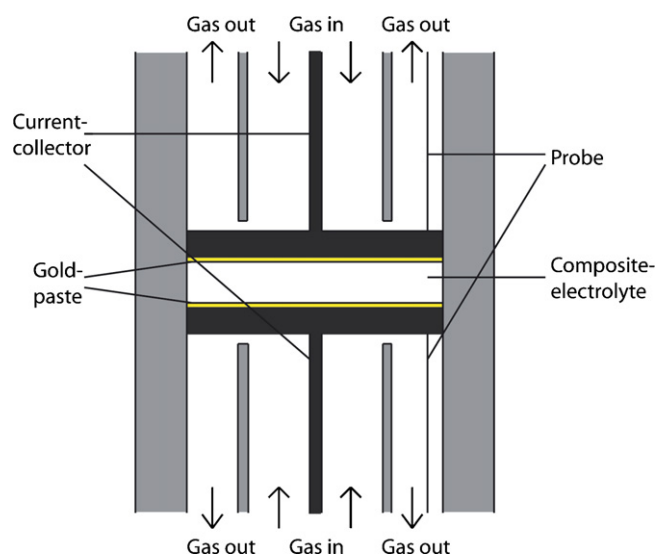

Fig. 1. Experimental setup of the electrolyte.

Table 2
Composition of anode gases used, vol.%

Anode gas	H_2	CO_2	N_2	CO
A1	80.0	20.0	0	0
A2	14.8	50.1	5.0	30.1

of the electrolyte was measured by a probe before and after each EIS measurement. The gas was changed and supplied continuously on both sides of the electrolyte. The flow was manually controlled and set to 10 ml min^{-1}. The different gas compositions used are shown in Tables 2 and 3. The gas was humidified in some cases; this was done by letting the gas bubble through water where the temperature was controlled.

For each experiment a composite electrolyte composition was chosen and the choice of anode gas or cathode gas environment was made. The conductivity of the pellet was measured both when going from low temperature (400 °C) to high temperature (700 °C), increasing temperature ramping, and vice versa, decreasing temperature ramping. When doing the experiments it was observed that a small difference in conductivity was recorded for a given sample, at about the same temperature, depending on increasing or decreasing temperature ramping. In order for the electrolyte temperature to stabilise between each experiment point, a longer period of time was needed when going down in temperature.

The EIS measurements were carried out using Solartron 1250 FRA and a Solartron 1287 potentiostat. The frequency spectra were recorded at open circuit potential (OCP) in the frequency range from 50 kHz to 30 mHz with an amplitude of 10 mV. The influence of the ac amplitude was tested before all the experiments were made to choose a value giving a stable response. The *z*-plot 2.8d software was used to measure and analyse the EIS data.

2.3. Methods for characterisation of the composites

X-ray diffraction (XRD) patterns of the composite electrolytes were recorded at room temperature using a PANalytical XPertPro using a Cu K$_\alpha$ radiation (1.54178 Å), 45 kV and 40 mA, with 2θ varying from 5° to 100°. The diffraction pattern was scanned in steps of 0.0167° with counting time varying in the range 10–60 s depending on sample.

Differential scanning calorimetry (DSC) analysis was performed on a Mettler-Toledo DSC820 equipped with a sample robot and a cryo cooler. The tests were made using a Mettler-Toledo high pressure gold plated steel crucible of 40 μl in N$_2$ atmosphere with a flow of 80 ml min^{-1}.

Table 3
Composition of cathode gases used, vol.%

Cathode gas	O_2	CO_2	N_2
C1	15.0	30.0	55.0
C2	15.1	69.9	15.0
C3	19.1	10.0	70.9
Air (synthetic)	21.0	0	79.0

The microstructures of both unused electrolyte pellets and used electrolyte pellets were characterised by scanning electron microscopy (SEM), using a JSM840, on the cross-section surface of the sample.

3. Results and discussion

3.1. Material properties

Fig. 2(a) shows the XRD patterns of pure SDC, a pure (Li/Na)$_2$CO$_3$ pellet and the different unused composites. Although not shown in the figure, (Li/Na)$_2$CO$_3$ powder and pure Sm$_2$O$_3$ powder were also tested as reference samples. The (Li/Na)$_2$CO$_3$ powder had the same pattern as the (Li/Na)$_2$CO$_3$ pellet but with more noise, while the Sm$_2$O$_3$ showed only one peak at 28°. The diffractogram from the unused pellets and the pure SDC powder show the same position and relative intensity for all peaks and it can be concluded that the structure of the solid oxide phase is not altered in the unused composite. The XRD pattern also indicates that the (Li/Na)$_2$CO$_3$ exists as an amor-
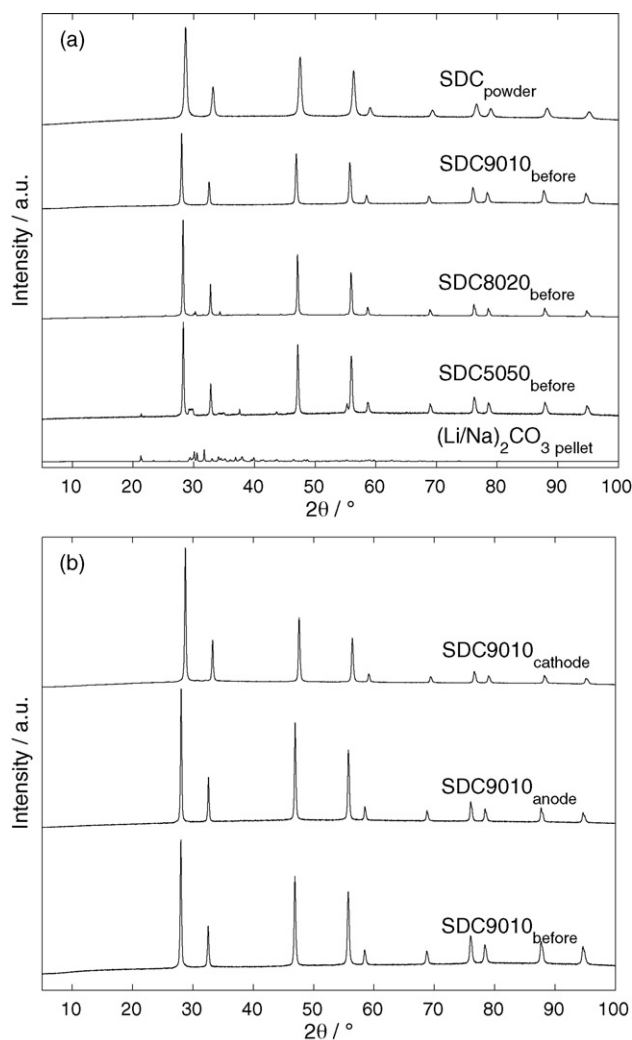

Fig. 2. XRD patterns. (a) SDC powder, (Li/Na)$_2$CO$_3$ pellet and the different unused composite pellets; (b) used and unused pellets for SDC9010.

phous phase in a coating over the SDC particles, as reported by other authors [8]. However, if comparing the diffractograms for SDC5050 and SDC8020 with that of the pure $(Li/Na)_2CO_3$ pellet some small peaks between $30°$ and $38°$ can be seen. These peaks indicate that some $(Li/Na)_2CO_3$ may be present in crystalline form. Fig. 2(b) show diffractograms of SDC9010 pellets used in cathode and anode environments compared to an unused electrolyte. According to the XRD patterns, the pellet is not influenced either by being used in reducing or in oxidising atmosphere. Also SDC8020 was tested in the same way showing the same patterns. The peaks seen in Fig. 2 have the same positions as in data given by Huang et al. [8], although they measured only up to $70°$. Comparing with the results from Zhu et al. [2] the same peak pattern and relative intensity are found. However, the positions of the peaks in data presented by Zhu et al. [2] are shifted in angle to more positive values and the last two peaks in Fig. 2 are not found in their measurement.

The surface morphologies of the unused electrolyte pellets, SDC5050, SDC8020 and SDC9010, sintered at $600°C$ were investigated by SEM. In Fig. 3(a) showing the composite SDC5050 the cross-section is smooth and the SDC seems to be distributed in the $(Li/Na)_2CO_3$ and larger crystals of $(Li/Na)_2CO_3$ are also observed. From the volume ratio of the different composites, presented in Table 1, it can be seen that the volume of $(Li/Na)_2CO_3$ in SDC5050 is three times larger than that of the oxide. In agreement with this, the SDC does not seem to form a continuous phase in the SEM picture. In Fig. 3(b), the two phases seem to be more evenly distributed and no clear interface is visible between the SDC and the $(Li/Na)_2CO_3$. The structure seems to consist of agglomerates. For SDC9010, Fig. 3(c), the structure is more homogeneous than for SDC8020 and larger agglomerates cannot be seen in the same way. The SEM micrographs show no larger pores in the structure for the three materials, but it cannot be excluded that sub-micrometer pores exist. The SEM study reveals that with an increasing amount of $(Li/Na)_2CO_3$, the surface becomes smoother, due to the larger amount of salt surrounding the SDC particles. For SDC8020 and SDC9010 SEM images were taken after usage in both anode gas and cathode gas environments. The cross-section surfaces look less rough than those of the unused pellets. The SEM images are similar to what Huang et al. [8] reported for their SDC-$(Li/K)_2CO_3$ composite electrolytes. In SEM images for the SDC9010 and SDC8020 samples no big carbonate crystals can be seen and this is in accordance with results for composites with lower weight fractions of carbonate salt reported by Huang et al. [8]. As regards the composite SDC5050, the SEM image is similar to what Huang et al. [8] show for their material with 45 wt.% carbonate, where larger carbonate crystals can be seen.

DSC measurements were performed on pure SDC, SDC8020 and $(Li/Na)_2CO_3$ powders and unused pellets of SDC8020 and SDC9010. All DSC results on samples containing $(Li/Na)_2CO_3$ show an endothermic phenomenon due to melting in the investigated temperature interval 20–550 $°C$. The DSC was measured twice, the first time it was concluded that the temperature sweep rate, $20°C\,min^{-1}$, strongly influenced the melting point peak position and for the second measurement the temperature sweep
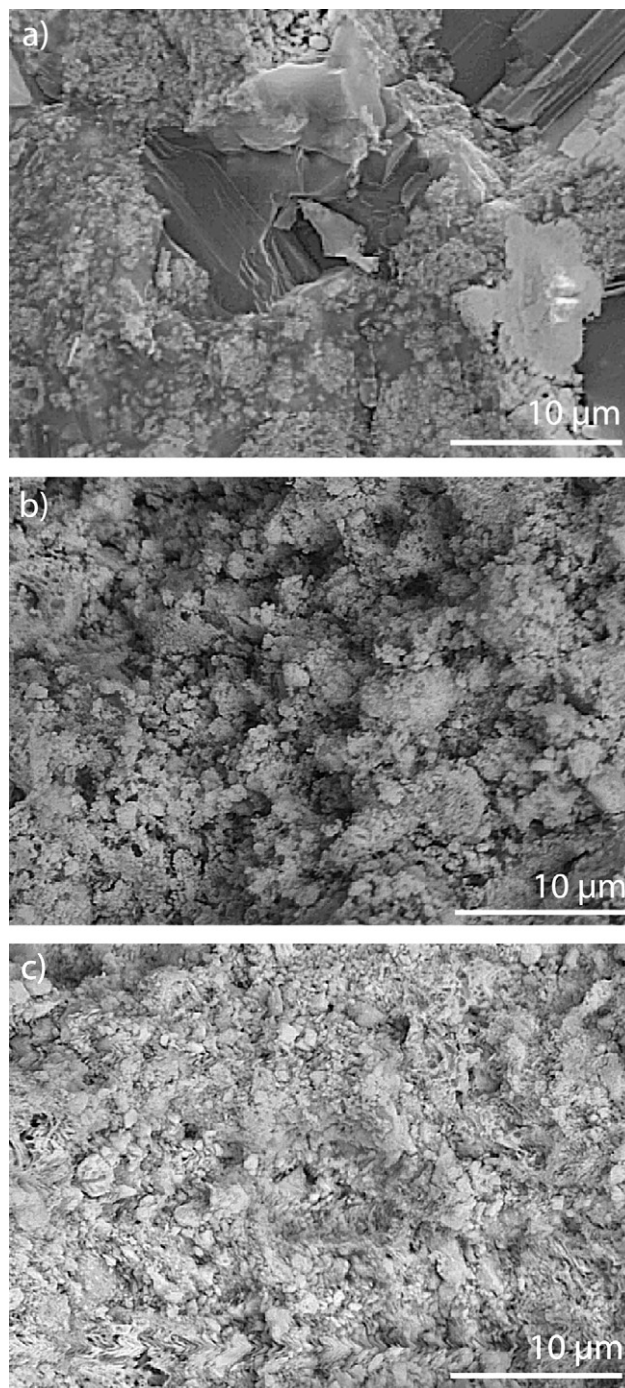

Fig. 3. SEM images of the cross-section surface before usage: (a) SDC5050, (b) SDC8020 and (c) SDC9010.

pattern was changed to $2°C\,min^{-1}$ in the temperature interval 450–550 $°C$ to get more accurate measurements. Fig. 4 shows the baseline-corrected DSC results, based on the weight of the $(Li/Na)_2CO_3$ in the sample, for the different samples tested in the temperature interval of interest. Fig. 4 shows that the SDC powder has no phase change in the temperature interval of interest (and not in the rest of the interval measured). It may also be seen from Fig. 4 that the melting of the $(Li/Na)_2CO_3$ phase starts at about the same temperature, 460–470 $°C$ for all the compos-
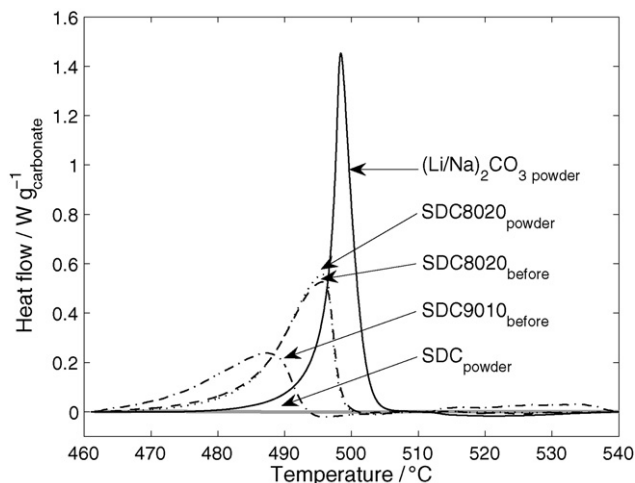
Fig. 4. DSC results. SDC, SDC8020 and $(Li/Na)_2CO_3$ powders and unused pellets of SDC9010 and SDC8020.

ites, but that the bulk melting point is lower for the composites than for the pure $(Li/Na)_2CO_3$ sample. The pure $(Li/Na)_2CO_3$ does show a lower degree of partial melting than the composites. Fig. 4 also shows that no changes occur with the composite when manufacturing the pellets from the powder for SDC8020. Moreover, it is clear from the figure that SDC9010 has a lower bulk melting point than has SDC8020. The pellets used for testing SDC8020 and SDC9010 were also tested after usage. A lower melting energy was observed for the used pellets compared to the unused and for some of the pellets also a small decrease in the bulk melting point was seen. Further study of the change of weight or melting energy of the used pellets is necessary before any clear conclusion may be reached. Including all the different DSC measurements one may conclude that the bulk melting temperature shifts towards lower temperature, with decreasing $(Li/Na)_2CO_3$ fraction. This phenomenon with decreasing melting point agrees with results from Mizuhata et al. [19] of Li_2CO_3 or K_2CO_3 coexisting with γ-$LiAlO_2$ or MgO. The DSC study also indicates that for the composites a partial melting of the $(Li/Na)_2CO_3$ occurs 10–20 °C before the melting point of the bulk.

3.2. Conductivity

The conductivities of SDC5050, SDC8020 and SDC9010 have been studied in various anode and cathode atmospheres for both dry and humidified gases. For all the pellets tested in the study it was observed that the first time a pellet was used it had lower conductivity below the $(Li/Na)_2CO_3$ melting point for the increasing temperature ramping than for the decreasing temperature ramping at the same temperature. The second time the same pellet was swept up and down in temperature this phenomenon does not occur. It was concluded that this is caused by the enhanced contact between the pellet and the current collector after $(Li/Na)_2CO_3$ is melted for the first time. No data from the first increasing temperature ramping are used in the analysis.

EIS data for the three composite electrolytes at two temperatures are given in Fig. 5 for gas A1. The measured EIS data

has been corrected for the surface area and the thickness of the pellet and is given in Ω cm to be consistent with the conductivity figures given afterwards. In Fig. 5, no typical semicircle is seen either below or above the $(Li/Na)_2CO_3$ melting point.

In Fig. 6, the Bode plots for the EIS data for SDC8020 run in air are shown at different temperatures. For the three impedance curves (a–c) below the melting point of $(Li/Na)_2CO_3$ it may be observed that the peak angle moves to higher frequencies with increasing temperature. This may also be seen for the three temperatures (e–g) above the melting point of $(Li/Na)_2CO_3$. It may also be seen that the frequency for the peak angle changes two orders of magnitude when going from a temperature below to above the melting point of the $(Li/Na)_2CO_3$. If the EIS data in Fig. 6 are illustrated in a Nyquist plot only one semicircle will appear. The EIS data for the three composites in all different
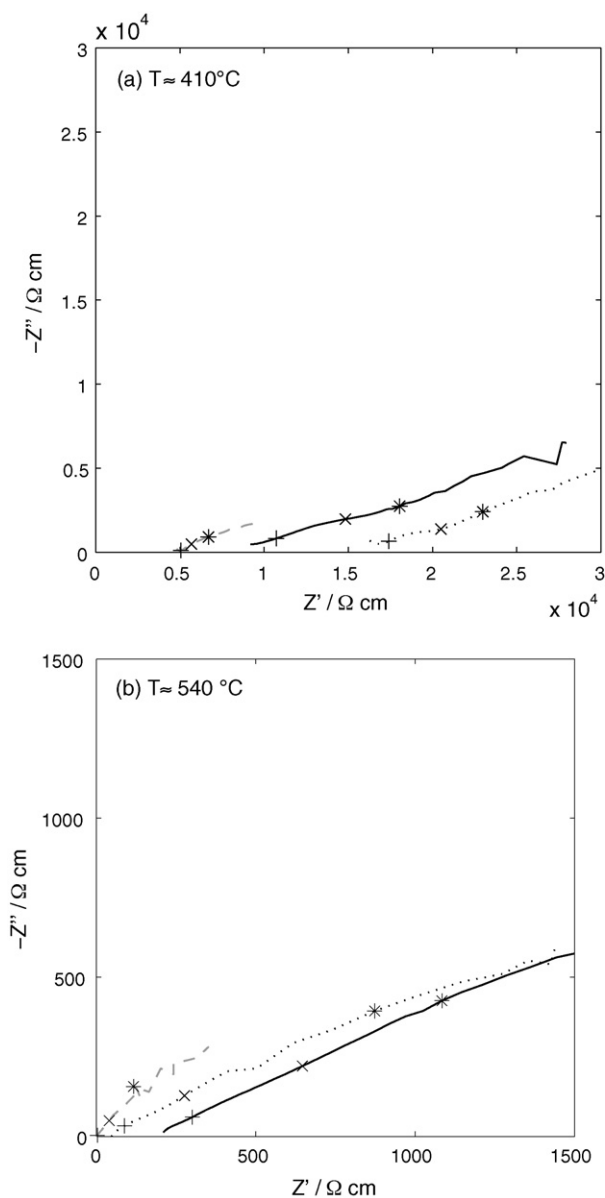

Fig. 5. (a and b) EIS data of the different composites for gas A1 (H_2/CO_2 80/20); (- - -) SDC5050, (—) SDC8020 and (· · ·) SDC9010. Marked frequencies: (+) 1000 Hz, ($\times$) 10 Hz and (*) 1 Hz.
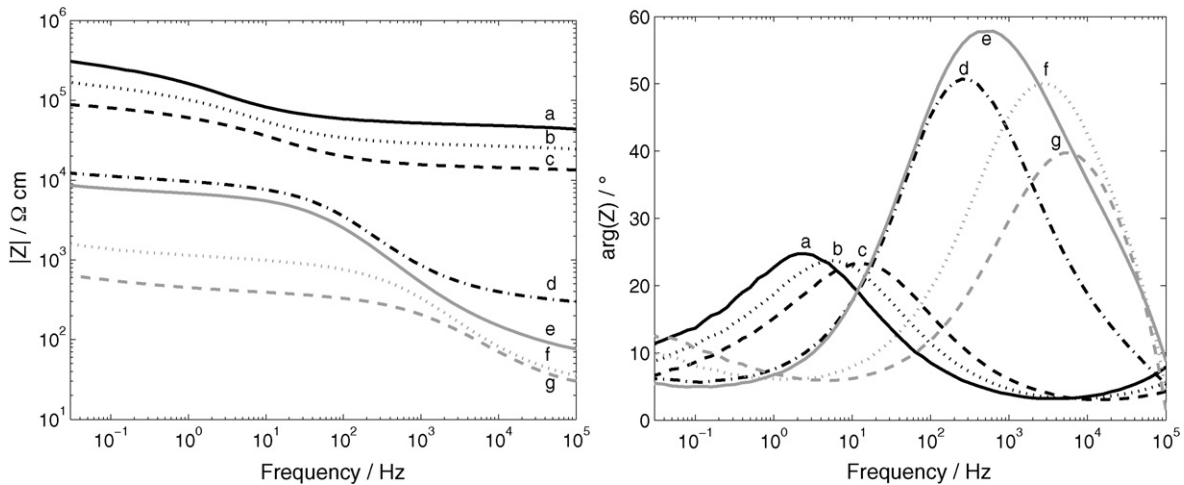
Fig. 6. EIS data for SDC8020 tested in air at different temperatures: (a) 402 °C, (b) 421 °C, (c) 443 °C, (d) 491 °C, (e) 516 °C, (f) 618 °C and (g) 707 °C.

cathode gases all show the same behaviour. The frequency of the peak of the semicircle is temperature dependent even below the melting point of $(Li/Na)_2CO_3$. This supports that the semicircle is caused by a charge transfer resistance in parallel with the double layer capacitance, and that the high-frequency intercept measures the bulk conductivity of the sample.

The conductivity was accordingly calculated from the high frequency intercept with the real axis in the EIS data. The dependency of the gas flow rate on the measured impedance was investigated before the experiments and it was concluded that the high frequency intercept was not affected by the gas flow rate. The impedance was measured both when going up and down in temperature. In all measurements two regions of the conductivity were observed, especially clearly shown for SDC5050 and SDC8020; one region below the melting temperature of $(Li/Na)_2CO_3$ and the other region above the melting temperature, see Fig. 7. The conductivities in the two different temperature regions are separated by a narrow zone where the conductivity changes dramatically. This zone has by other authors [7,8,20] been explained by the existence of a superionic phase. This superionic phase may be formed between two conducting phases, forming a space charge region, according to Maier [21]. That the conductivity of a carbonate salt has two regions has also been reported by Mizuhata et al. [19] for Li_2CO_3 or K_2CO_3 coexisting with γ-$LiAlO_2$ or MgO. Despite only having the carbonate salt as conducting phase their study shows conductivity even below the bulk melting point of the salt. Following from the DSC results presented here, the sudden improvement of the conductivity in this zone most probably depends on the $(Li/Na)_2CO_3$ being in contact with the DCO particles partially melting below the bulk melting point. This partial melting is enough to enhance the conductivity, since also the $(Li/Na)_2CO_3$ phase may be used for ion conduction.

When comparing the effect of the two different anode gases on SDC9010 it was observed that the conductivity in the hydrogen-rich gas was slightly larger above the melting point, see Fig. 8(a). The same behaviour was also observed for SDC5050. Below the melting point the conductivity in gas A1 compared to gas A2 was lower for SDC9010, while conductiv-
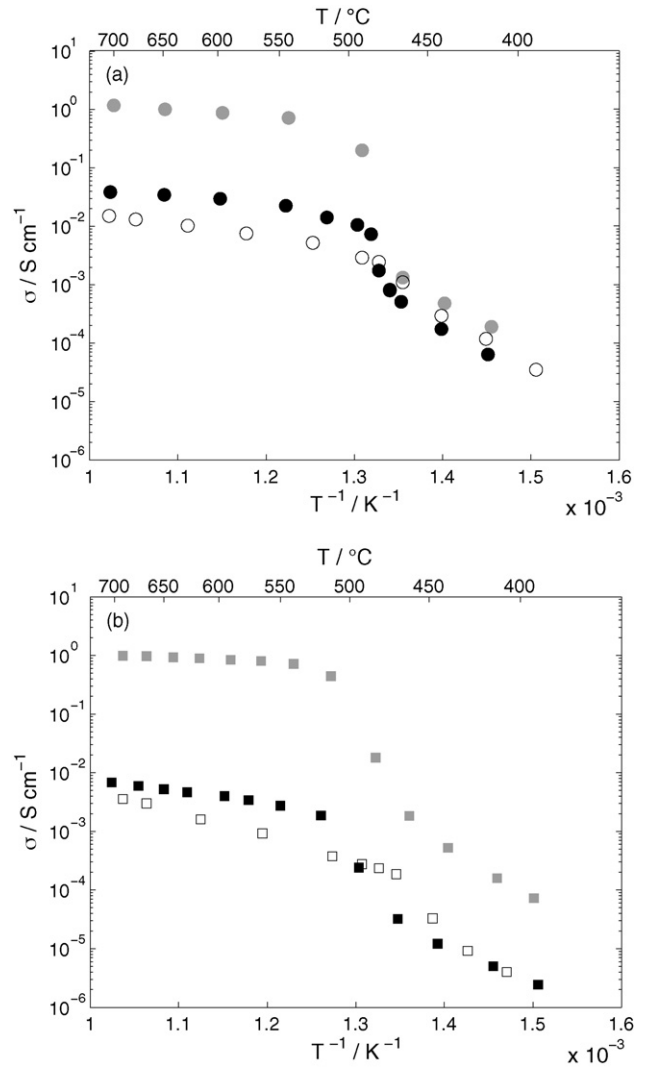

Fig. 7. Conductivity of different composites. (a) Gas A1 (H_2/CO_2 80/20): (●) SDC5050, (●) SDC8020 and (○) SDC9010; (b) gas C3 ($O_2/CO_2/N_2$ 19/10/71): (■) SDC5050, (■) SDC8020 and (□) SDC9010.

ities were the same for SDC5050. In Fig. 8(b), the conductivity in gases C1 and C2 seems to be higher, especially at lower temperature, than that in gas C3. However, no large difference can be seen between the different cathode gases. This indicates that the conductivity is not strongly dependent on the oxygen partial pressure. Neither does the difference in CO_2 content between gas C1 and C2 affect the conductivity noticeably.

In Figs. 7 and 8, it may be seen that the conductivity of SDC8020 and SDC9010 in anode gases are 5–10 times larger than in cathode gases for the whole temperature range. This may be caused by the reduction of Ce^{4+} to Ce^{3+} in reducing atmosphere (anode environment), leading also to electronic conduction [4,5]. This redox pair has also been observed by Cassir and co-workers [22,23] for CeO_2 coexisting with $(Li/Na)_2CO_3$. They also reported that Ce^{4+} has some solubility in the salt phase. For SDC5050 the higher conductivity in anode gas cannot be observed. The SDC5050 composite shows the highest conductivity in the whole temperature region, Fig. 7. This result points to a very positive effect of the carbonate phase even when
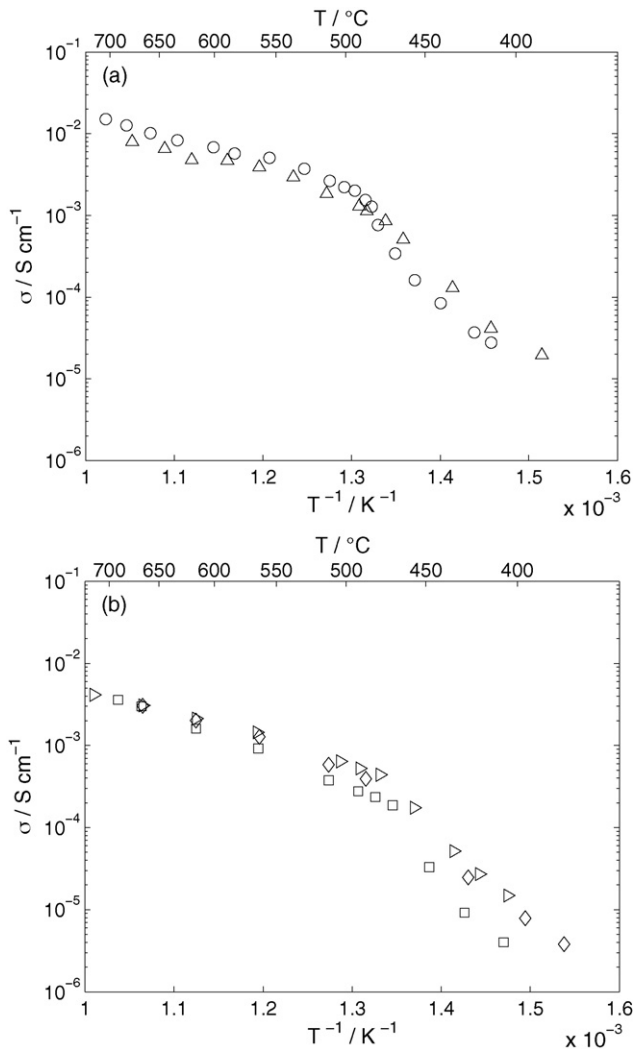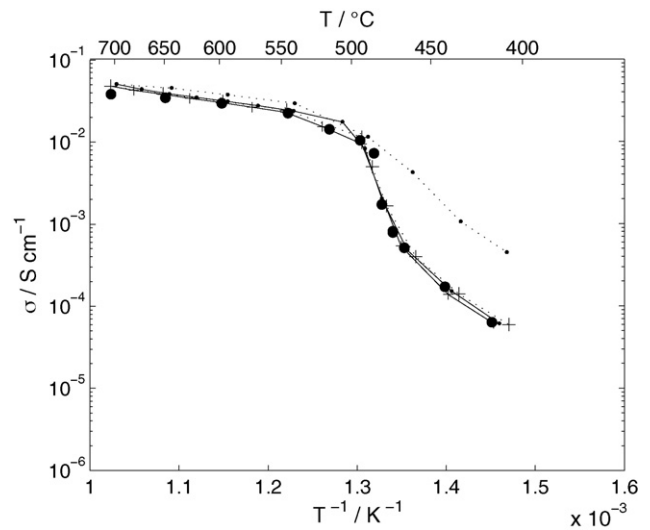

Fig. 9. Conductivities of SDC8020 for (—) increasing temperature ramping and (- - -) decreasing temperature ramping for gas A1 (H_2/CO_2 80/20): (●) dry, (+) 2% humidified and (•) 7% humidified.

being in its solid phase, at least when present in such large amount.

The effect of humidification of the gases on the conductivity of the composites was tested. In Fig. 9 data for SDC8020 with gas A1 are presented. This shows that the conductivity is increasing a little already when humidifying the gas with 2% water. This behaviour was also observed for SDC9010, but could not be so clearly seen for SDC5050. Increasing the humidification further to 7% did not affect the conductivity to any larger extent. However, an interesting phenomenon was observed for the SDC5050 and SDC8020 samples (Fig. 9) at 7% humidification in both anode and cathode gas. In the decreasing temperature, ramping the conductivity is much larger than when increasing the temperature, especially for temperatures below the $(Li/Na)_2CO_3$ melting point. The same behaviour was also observed for gas C3.

Humidifying the gases leads to at least a slightly improved conductivity for all the different composites. The largest improvement of the conductivity is observed for SDC9010 with gas A2, where it is approximately doubled. An explanation for the increased conductivity is that the humidified gas enables some formation of hydroxides from $(Li/Na)_2CO_3$. The extent of hydroxide formation depends on the equilibrium between the different species in the electrolyte and in the gas [18,24]. If hydroxides are formed in the electrolyte they will lower the melting point and increase the conductivity [20].

In Fig. 10, the conductivity of SDC8020 run in air, both dry and 2% humidified, is compared with the conductivity in gases A1 and C3. Two different tests were made in air with the same pellet. During the first test, the pellet was run in open air (without any forced flow). The second time the pellet was tested under the same conditions as all the other pellets, except that the pellet was cycled in temperature up to 650 °C and down again before the measurement was started. In the first test, the conductivity of the pellet in dry air is comparable to that in gas A1, especially at temperatures above the $(Li/Na)_2CO_3$ melting point. However, in
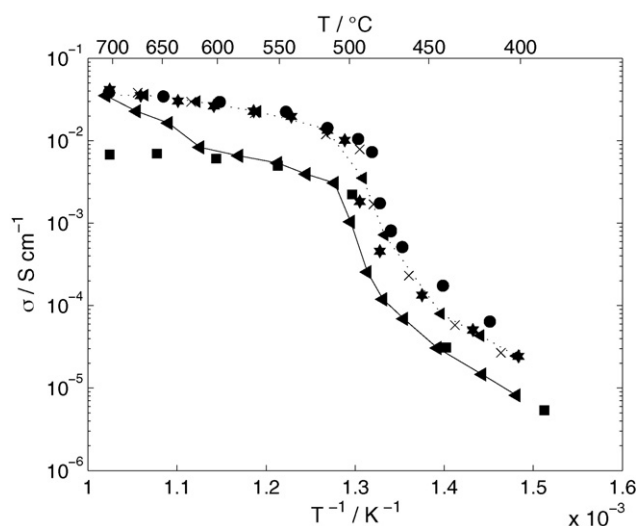

Fig. 8. Conductivities of SDC9010: (a) (○) gas A1 (H_2/CO_2 80/20) and (△) gas A2 ($H_2/CO_2/N_2/CO$ 15/50/5/30). (b) (◇) gas C1 ($O_2/CO_2/N_2$ 15/30/55), (▷) gas C2 ($O_2/CO_2/N_2$ 15/70/15) and (□) gas C3 ($O_2/CO_2/N_2$ 19/10/71).

Fig. 10. Conductivity of SDC8020 in air compared to anode gas and cathode gas: (●) gas A1 (H_2/CO_2 80/20), (■) gas C3 ($O_2/CO_2/N_2$ 19/10/71), (×) air dry first test, (–◀–) air dry second test increasing temperature ramping, (···◀···) air dry second test decreasing temperature ramping and (✦) air 2% humidified second test increasing temperature ramping.

the second test the conductivity in dry air is about the same as in gas C3 for the increasing temperature sweep, but at 600 °C the conductivity suddenly improves and at 700 °C it is the same as in gas A1. For the decreasing temperature ramping, the conductivity in dry air is as in the first test, similar to that in gas A1 for the whole temperature interval. The difference between the increasing and decreasing temperature ramping is strange since the pellet was swept once already before the measurements started. For the humidified air there is no large difference seen between the increasing and decreasing temperature ramping. With one exception, all the experiments in air, when compared to experiments in gas C3, seem to result in better conductivities for the electrolyte. However, it is difficult to tell what factor is the cause of the improving effect. The oxygen content is somewhat higher in air than in gas C3, which may have a beneficial effect. The largest difference though is the amount of carbon dioxide, 10% in gas C3, while negligible in air. Comparing results from air and gas C3 measurements, points at a very negative effect on the electrolyte conductivity from CO_2. However, the amount of CO_2 is even higher (20%) in the anode gas A1 and the electrolyte conductivity is in this case as good as in air. Therefore, the CO_2 content does not seem to affect the conductivity to a large extent, which was also shown in Fig. 8 for both anode and cathode gases. In any way some carbon dioxide is always needed in order to keep the stability of the melt, but according to present results CO_2 content may be kept very low.

The conductivity of SDC8020 tested in air is compared to literature data in Fig. 11 (summarised in Table 4). From the graph it is found that SDC8020 and Electrolyte 3 show about the same pattern with a transition in conductivity value at around 500 °C, but that SDC8020 has a lower conductivity throughout the whole temperature range tested. One difference between the two electrolytes is the carbonate mixture used. $(Li/Na)_2CO_3$ is used in the SDC8020, but this is not likely to influence notice-

Table 4
Some electrolytes from literature tested in air.

Name	Composite	Reference
Electrolyte 1	80 wt.% SDC-20 wt.% $(Li/K)_2CO_3$ (62/38 mol%)	[8]
Electrolyte 2	GDC-$(Li/K)_2CO_3$	[6]
Electrolyte 3	80 wt.% SDC-20 wt.% $(Li/K)_2CO_3$ (62/38 mol%)[a]	[7]
Electrolyte 4	SDC	[7]

[a] The original ratio is 50 vol.% SDC-50 vol.% $(Li/K)_2CO_3$ (62/38 mol%) has been recalculated to weight ratio for comparison.

ably on the measured conductivity. A possible reason for the different conductivities observed may instead be that different experimental setups are used. In experiments with Electrolyte 3 presented by Zhu et al. [7] also electrodes were added, while in the present paper only the electrolyte was put between two current collectors. In comparison with Electrolyte 1, also having the same oxide/carbonate weight ratio, SDC8020 has a higher conductivity above the carbonate melting point, while its conductivity below that point is 10–100 times lower. The conductivity behaviour of Electrolyte 1 shows a very clear plateau at higher temperatures and the transition between the two regions seems to occur at a surprisingly low temperature compared to the melting point of the pure salt phase. Electrolyte 2 with GDC shows the highest conductivity. Unfortunately, it is only studied in a very narrow temperature range making the comparison with other composites in the graph unfair. The conductivity of the pure SDC electrolyte increases almost linearly with increasing temperature throughout the whole temperature interval 400–550 °C. This electrolyte does not include any carbonate and accordingly no transition region due to carbonate melting is found. Judging from the data presented in Fig. 11, a fuel cell operating below the melting temperature of the carbonate salt, should be best off with an electrolyte consisting of pure SDC, while composites are better at higher temperatures.
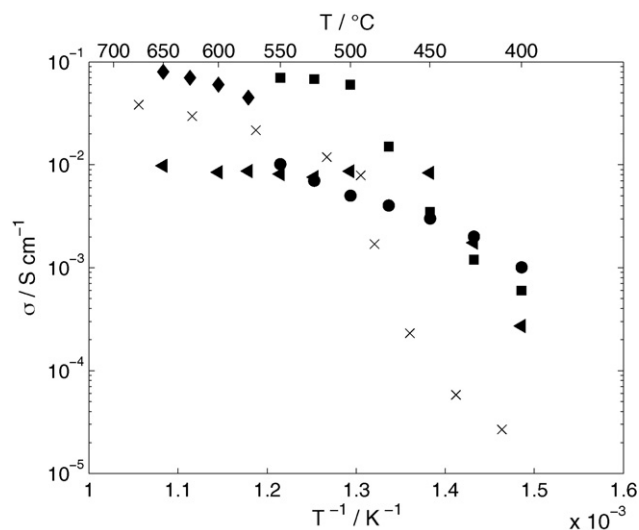

Fig. 11. SDC8020 used in air compared to literature data. (×) SDC8020, (◀) Electrolyte 1, (◆) Electrolyte 2, (■) Electrolyte 3 and (●) Electrolyte 4.

Table 5
Calculated activation energies for the different composites

Sample	Gas	Temperature region (°C)	Activation energy		Conductivity (S cm^{-1})	
			kJ mol^{-1}	eV	440 (°C)	650 (°C)
SDC5050	A1	550–700	19	0.20		2.6
		389–450	141	1.47	4.8×10^{-4}	
SDC5050	C3	565–691	11	0.11		1.1
		393–462	189	1.70	5.3×10^{-4}	
SDC8020	A1	544–703	38	0.40		3.4×10^{-2}
		410–465	175	1.83	1.4×10^{-4}	
SDC8020	C3	550–703	39	0.40		5.2×10^{-3}
		391–469	133	1.38	1.2×10^{-5}	
SDC8020	Air	570–700	36	0.38		2.2×10^{-3}
		400–460	149	1.55	5.8×10^{-5}	
SDC9010	A1	576–700	37	0.38		6.8×10^{-3}
		394–442	164	1.71	8.0×10^{-5}	
SDC9010	C3	550–717	48	0.50		2.1×10^{-3}
		405–450	196	2.04	3.3×10^{-5}	

The conductivity as a function of volume fraction carbonate salt, $(Li/Na)_2CO_3$, of the different composite compositions tested as well as conductivities of pure $(Li/Na)_2CO_3$ and pure SDC are shown in Fig. 12. It may be seen that the conductivity dependency of the carbonate volume fraction increases with increasing amount of carbonate for all gases tested in this study. For cathode gases, the conductivity of SDC8020 and SDC9010 is lower than that reported by Zhu et al. [7] for pure SDC tested in air. But for the same electrolyte tested in anode gases, the conductivity is about the same as for the pure SDC. A theory for percolating phases indicates that at about 30% volume fraction of a phase it starts to be continuous [25]. Zhu et al. [7] tested the carbonate volume fraction dependency of SDC-$(Li/K)_2CO_3$ and had a large change in conductivity at about 30 vol.%.
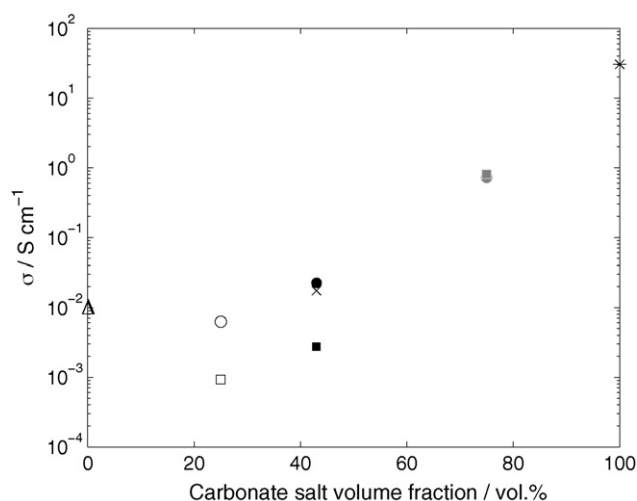

Fig. 12. The conductivity of the composite electrolytes as a function of the volume fraction of the carbonate salt at 550 °C, in both anode gas (squares), cathode gas (circles) and air (×). (□ and ○) SDC9010, (■, ● and ×) SDC8020, (▨ and ●) SDC5050; (*) pure $(Li/Na)_2CO_3$ [18] and (△) pure SDC tested in air [7].

The activation energies for the conductivity were calculated for the different composite compositions for one anode gas and one cathode gas, above and below the melting point of $(Li/Na)_2CO_3$ (Table 5). As may be seen for the temperature region above the melting point of $(Li/Na)_2CO_3$ the activation energy is about 0.4 eV except for SDC5050. However, below the melting point the values vary more both for the same composition with different gases and between the different composites. The number of data points below the melting point is small and this makes the value of the activation energy less accurate. There is no clear trend or specific value of the activation energy that would indicate a certain transport mechanism for the ion conduction in these different composites or in the different gas compositions. Comparing the activation energies in Table 5 with data reported by Schober [20], where the activation energy was 0.5 eV above the melting point and 1.3 eV below the melting point in dry and humidified air, respectively, it is found that the data for SDC8020 in air is lower above the melting point and higher below the melting point, resulting in a larger difference between the two values.

4. Conclusions

In this work, composite electrolytes with different weight fractions of SDC and $(Li/Na)_2CO_3$ were studied by EIS, XRD, DSC and SEM. Conductivity of the composite electrolyte pellets was tested in both gaseous anode and cathode atmospheres. Results from XRD shows that no changes occur to the structure of the oxide phase either for electrolytes tested in reducing or in oxidising atmosphere.

The SEM images show a good mixture of the two different phases for SDC9010 and SDC8020, but for SDC5050 larger $(Li/Na)_2CO_3$ crystals were observed and the SDC seems to be evenly distributed in the $(Li/Na)_2CO_3$ without forming a percolating phase. The used pellets show a smoother surface when compared to the unused pellets.

For all the composites, two regions may be observed for the conductivity, one below the $(Li/Na)_2CO_3$ melting point and one above melting point. A transition region may also be observed, especially for SDC5050 and SDC8020; it is probably due to partial melting of $(Li/Na)_2CO_3$. The conductivity is enhanced in the high temperature region with increasing amount of $(Li/Na)_2CO_3$ phase for both anode gases and cathode gases. DSC shows that partial melting of $(Li/Na)_2CO_3$ starts about 10–20 °C before the bulk melting point and that the bulk melting point decreases with decreasing amount of $(Li/Na)_2CO_3$ phase.

The conductivity in anode gases was found to be 5–10 times larger than in cathode gases for SDC8020 and SDC9010 above the melting point of $(Li/Na)_2CO_3$. Conductivities in air are similar to the conductivities in anode gas A1 and higher than in cathode gas C3. The difference between the cathode gas and the air is that the carbon dioxide content is about 10% in gas C3. Since the anode gas A1 contains even more carbon dioxide than gas C3, about 20%, the better conductivity of air-run electrolyte is probably not due to the low CO_2 content. The content of CO_2 and O_2 does not seem to strongly affect the conductivity.

Calculations of the activation energies for the conductivity show no value or trend in value between the different composites or for the different gases tested and no mechanism for ion transport can be concluded.

Acknowledgements

References

[1] T. Tsai, E. Perry, S. Barnett, J. Electrochem. Soc. 144 (1997) L130–L132.
[2] B. Zhu, X.T. Yang, J. Xu, Z.G. Zhu, S.J. Ji, M.T. Sun, J.C. Sun, J. Power Sources 118 (2003) 47–53.
[3] B. Zhu, X. Liu, T. Schober, Electrochem. Commun. 6 (2004) 378–383.
[4] B.C.H. Steele, Solid State Ionics 129 (2000) 95–110.
[5] A. Atkinson, Solid State Ionics 95 (1997) 249–258.
[6] G.Y. Meng, Q.X. Fu, S.W. Zha, C.R. Xia, X.Q. Lu, D.K. Peng, Solid State Ionics 148 (2002) 533–537.
[7] W. Zhu, C. Xia, D. Ding, X. Shi, G. Meng, Mater. Res. Bull. 41 (2006) 2057–2064.
[8] J. Huang, Z. Mao, L. Yang, R. Peng, Electrochem. Solid-State Lett. 8 (9) (2005) A437–A440.
[9] J.B. Huang, L. Yang, R. Gao, Z. Mao, C. Wang, Electrochem. Commun. 8 (2006) 785–789.
[10] Q.X. Fu, S.W. Zha, W. Zhang, D.K. Peng, G.Y. Meng, B. Zhu, J. Power Sources 104 (2002) 73–78.
[11] B. Zhu, X. Liu, P. Zhou, X. Yang, Z. Zhu, W. Zhu, Electrochem. Commun. 3 (2001) 566–571.
[12] J. Hu, S. Tosts, Z. Guo, Y. Wang, J. Power Sources 154 (2006) 106–114.
[13] B. Zhu, J. Power Sources 114 (2003) 1–9.
[14] B. Zhu, I. Albinsson, C. Andersson, K. Borsand, M. Nilsson, B.-E. Mellander, Electrochem. Commun. 8 (2005) 498.
[15] J. Liu, A.C. Co, S. Paulson, V.I. Birss, Solid State Ionics 177 (2006) 377–387.
[16] Y.F. Gu, G. Li, G.Y. Meng, Mater. Res. Bull. 35 (2000) 297–304.
[17] J.A. Dean, Lange's Handbook of Chemistry, 11th ed., McGraw-Hill, New York, 1973 (Section 9.3).
[18] J.R. Selman, H.C. Maru, Physical Chemistry and Electrochemistry of Alkali Carbonate Melts in Advances in Molten-Salt Chemistry, vol. 4, Plenum Press, New York, 1981, pp. 159–361.
[19] M. Mizuhata, Y. Haranda, G.-J. Cha, A.B. Béléke, S. Deki, J. Electrochem. Soc. 151 (2004) E179–E185.
[20] T. Schober, Electrochem. Solid-State Lett. 8 (4) (2005) A199–A200.
[21] J. Maier, Prog. Solid State Chem. 23 (1995) 171–263.
[22] V. Chauvaut, V. Albin, H. Schneider, M. Cassir, H. Ardéléan, A. Galtayores, J. Appl. Electrochem. 30 (2000) 1405–1413.
[23] M. Cassir, V. Chauvaut, V. Alfarra, V. Albin, J. Appl. Electrochem. 30 (2000) 1415–1420.
[24] K. Suguira, T. Yodo, M. Yamauchi, K. Tanimoto, J. Power Sources 157 (2006) 739–744.
[25] Z. Wu, M. Liu, Solid State Ionics 93 (1996) 65–84.